RSC Advances

PAPER

View Article Online
View Journal | View Issue

Check for updates

Cite this: *RSC Adv.*, 2017, **7**, 49031

Factors influencing fast ion transport in glyme-based electrolytes for rechargeable lithium–air batteries†

Morihiro Saito, *[a] Shinya Yamada,[a] Taro Ishikawa,[a] Hiromi Otsuka,[b] Kimihiko Ito[b] and Yoshimi Kubo [b]

Received 7th July 2017
Accepted 1st October 2017

DOI: 10.1039/c7ra07501d

rsc.li/rsc-advances

To elucidate the determination factors affecting Li-ion transport in glyme-based electrolytes, six kinds of 1.0 M tetraglyme (G4) electrolytes were prepared containing a Li salt ($LiSO_3CF_3$, $LiN(SO_2CF_3)_2$, or $LiN(SO_2F)_2$) or different concentrations (0.5, 2.0, or 2.7 M) of $LiN(SO_2CF_3)_2$. In addition to conventional bulk parameters such as ionic conductivity (σ), viscosity (η), and density, self-diffusion coefficients of Li^+, anions, and G4 were measured by pulsed-gradient spin-echo nuclear magnetic resonance method. Interaction energies (ΔE) were determined by density functional theory calculations based on the supermolecule method for Li^+–anion (salt dissociation) and G4–Li^+ (Li^+ solvation) interactions. The ΔE values corresponded to ion diffusion radii formed by solvation and/or ion pairs. The order of dissociation energies ΔE was $LiSO_3CF_3$ > $LiN(SO_2CF_3)_2$ > $LiN(SO_2F)_2$, which agreed well with the dissociation degree of these salts in the electrolytes. From the obtained knowledge, we also demonstrated that increasing the mobility and number of carrier ions are effective ways to enhance σ of glyme-based electrolytes by using 1,2-dimethoxyethane with lower η and similar dielectric constant to those of G4.

Introduction

In recent years, lithium–air batteries (LABs) with non-aqueous electrolytes have attracted much attention as large-scale energy storage devices for electric vehicles and stationary energy storage systems because of their high theoretical specific energy of 3505 Wh kg^{-1}, which is *ca.* nine times larger than that of conventional lithium-ion batteries (LIBs) (387 Wh kg^{-1}).[1] The first LAB system was reported by Abraham and co-workers, and recently many researchers have devoted intense effort to improving LAB cell performance.[2] Initially, organic carbonate solvents such as propylene carbonate (PC), ethylene carbonate (EC), and diethyl carbonate (DEC) were used in LABs because of their low volatility, compatibility with lithium (Li) metal and high oxidation stability over 4.5 V *vs.* Li/Li^+. However, these organic carbonate-based electrolytes were found to be readily decomposed by the superoxide (O_2^-) radicals formed during the discharge process,[3–6] and $C_3H_8(OCO_2Li_2)$, Li_2CO_3, HCO_2Li, CH_3CO_2Li, CO_2, and H_2O were generated as by-products of Li_2O_2 formation.[7] Recently, ether-based electrolytes using 1,2 dimethoxyethane (DME or G1), diglyme (G2), triglyme (G3), or tetraglyme (G4) as a solvent have been widely investigated for non-aqueous LAB systems.[8] These ethers have high oxygen solubility and relatively low electric constants, resulting in lower reactivity toward O_2^- radicals compared with that of carbonate-based electrolytes.[9] Also, Li_2O_2 formation was confirmed after discharge. However, G1 and G2 are not suitable for practical use because of their high vapor pressure at room temperature. Instead, G4-based electrolytes containing Li salts such as $LiSO_3CF_3$ (LiOTf) and $LiN(SO_2CF_3)_2$ (LiTFSI) are commonly used in LAB research. Recent studies have revealed that the glyme-based electrolytes are decomposed by O_2^- radicals, especially in the charge process, and form Li_2CO_3, HCO_2Li, and CH_3CO_2Li in a similar manner to organic carbonate-based electrolytes.[10,11] As a result, the round-trip efficiency of O_2 for LABs is still low (*ca.* 60%), so glymes are not optimal electrolytes for non-aqueous LAB systems.[1,12] However, glyme-based electrolytes are still one of the better candidates for LAB systems because most other electrolytes decompose under the severe operating conditions. If the overpotential for electrochemical oxidation of Li_2O_2 could be lowered, it may be possible to use glyme-based electrolytes. For this purpose, some mediators such as LiI and LiBr have recently been applied to glyme-based electrolytes to promote Li_2O_2 oxidation at the air electrode.[13–16] Meanwhile, to suppress Li dendrite growth at the Li metal negative electrode (NE), a new inorganic Li salt, *i.e.*, $LiNO_3$, has been applied to glyme-based electrolytes to

[a]*Department of Applied Chemistry, Faculty of Engineering, Tokyo University of Agriculture & Technology, 2-24-16 Naka-cho, Koganei-shi, Tokyo 184-8588, Japan. E-mail: mosaito@cc.tuat.ac.jp; Fax: +81-42-388-7095; Tel: +81-42-388-7095*

[b]*GREEN, National Institute for Materials Science (NIMS), 1-1 Namiki, Tsukuba 305-044, Japan*

† Electronic supplementary information (ESI) available. See DOI: 10.1039/c7ra07501d

Open Access Article. Published on 18 October 2017. Downloaded on 6/14/2026 12:01:09 PM.
This article is licensed under a Creative Commons Attribution-NonCommercial 3.0 Unported Licence.

Open Access Article. Published on 18 October 2017. Downloaded on 6/14/2026 12:01:09 PM.
This article is licensed under a Creative Commons Attribution-NonCommercial 3.0 Unported Licence.

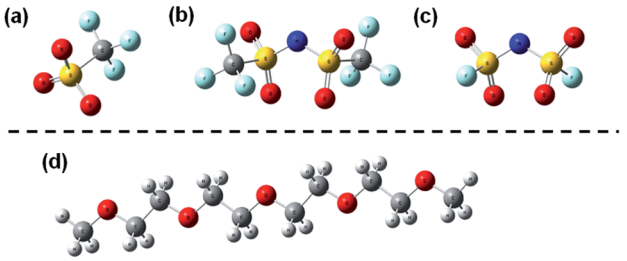

Fig. 1 Chemical structures of the anions and G4 used in this study, as optimized by DFT calculation using the B3LYP/6-311+G** basis set. (a) $CF_3SO_3^-$ (OTf^-), (b) $N(SO_2CF_3)_2^-$ ($TFSI^-$), (c) $N(SO_2F)_2^-$ (FSI^-), and (d) tetraglyme (G4). Red: O, yellow: S, light blue: F, gray: C, dark blue: N, and white: H.

stabilize the surface by oxidation.[17,18] Therefore, glyme-based electrolytes are still important materials for LAB systems.

Watanabe *et al.*[19,20] developed concentrated Li salt glyme-based electrolytes, called solvate ionic liquids, for LAB and Li–S battery systems. These electrolytes displayed interesting properties such as quite low solubility of polysulfide lithium and high electrochemical stability derived from the strong interaction between Li^+ and glyme (G3, G4) solvents. Both battery systems containing the solvate ionic liquids demonstrated stable cell performance. Concerning such concentrated Li salt electrolyte systems, Qian and colleagues reported that concentrated $LiN(SO_2F_3)_2$ (LiFSI) salt DME-based electrolytes exhibited a highly efficient Li dissolution/deposition reaction at a Li metal NE without Li dendrite growth.[21] This also suggests a new possibility for glyme-based electrolytes. Therefore, to develop new electrolytes and the next-generation battery systems, further research on glyme-based electrolytes is also important to help realize fast ion transport.

In this study, we prepared six glyme-based electrolytes with different Li salts (LiOTf, LiTFSI, and LiFSI) and a common salt LiTFSI with different concentrations for recent LABs. Fig. 1 shows the chemical structures of anions and G4 used in this study. We measured the individual self-diffusion coefficients D of the ions and G4 solvent in the glyme-based electrolytes by pulsed-gradient spin-echo nuclear magnetic resonance (PGSE-NMR) method, together with conventional physical properties, *i.e.*, ionic conductivity σ, viscosity η and density d, of the electrolytes to clarify their Li^+ transport behavior. The relationships between D and the other conventional properties are analyzed and discussed especially from the viewpoint of the mobility μ and number n of carrier ions in the electrolytes. To elucidate the relationship between the interactions between the chemical species and Li^+ transport behavior in the electrolytes, we also estimated the interaction energies between Li^+–anion and G4–Li^+ by density functional theory (DFT) calculations based on the supermolecule method[22,23] for each electrolyte system. Moreover, from the obtained knowledge, we proposed two strategies for glyme-based electrolytes to enhance ionic conductivity through increasing μ and n by using G1 as a solvent, and demonstrated the concepts to improve Li^+ transport in the electrolytes for LAB systems.

Experimental

To prepare glyme-based electrolytes for LABs, LiOTf (99.0%, Kishida) and LiTFSI (99.9%, Kishida) and LiFSI (99.0%, Kishida) were used as supporting salts, dissolved in G4 (Japan Advanced Chemicals, H_2O content: <30 ppm) as a solvent overnight in an Ar-filled dry box (GBJF100E805, Glovebox Japan Inc.), and aged for a few days.

σ of the electrolytes was measured by a conductivity meter (S230 SevenCompact, Mettler Toledo) in the temperature range of 303 to 333 K at 10 K intervals. The electrolytes were thermally equilibrated at each temperature for at least 1 h prior to measurement.

The D values of the Li^+ (^7Li), anion (^{19}F), and solvent G4 (^1H) in the electrolytes were measured by PGSE-NMR using a JEOL tunable pulsed-field gradient (PFG) probe (^1H resonance: 400 MHz) between 303 and 333 K.[24–28] Each sample was prepared in an NMR microtube (BMS-005J, Shigemi, Tokyo) to a height less than 5 mm to prevent convection effects. The PFG was calibrated using H_2O (^1H resonance). Measurements were performed by setting the same PFG strength for each nuclear species with different irradiation times δ. The accuracy of D values was confirmed by obtaining the same values at different δ.

Measurements of η and ρ were carried out using a Falling ball-type viscometer (Lovis2000ME, Anton Paar). The temperature was controlled in the range of 303 to 333 K at 10 K intervals while heating the samples.

The Li^+–anion and G4–Li^+ interactions were quantitatively investigated by DFT calculations performed using Gaussian 09 software.[29] The geometries of anions, G4, and their complexes were optimized by DFT using the B3LYP form for the exchange–correlation function and the 6-311+G** basis set. From results of the total electron energy of the ions, solvent, and complexes by the same basis set, the Li^+–anion and G4–Li^+ interaction energies ΔE were calculated by the supermolecule method.[22,23] The basis set superposition error (BSSE)[30] was corrected for all the interaction energy calculations using the counterpoise method.[31]

Results

Fig. 2(a) and (b) show the temperature dependences of σ for 1.0 M G4-based electrolytes with three kinds of Li salts with different anions (OTf^-, $TFSI^-$, and FSI^-) and the common Li salt LiTFSI at different concentrations (0.5, 1.0, 2.0, and 2.7 M), respectively. All plots veered slightly towards higher values, but approximately followed Arrhenius-type behavior. For the different anions, σ decreased with the order of LiFSI $\geq$ LiTFSI $\gg$ LiOTf across the entire temperature range from 303 to 333 K. σ of the LiOTf-based electrolyte was almost one order of magnitude lower than those of the other Li salt-based ones. On the other hand, focusing on the Li salt concentration, σ changed with the order of 1.0 M > 2.0 M > 2.7 M > 0.5 M at 60 °C, and σ of the higher concentration electrolytes (2.0 and 2.7 M) decreased relatively rapidly as the temperature lowered. These differences will be discussed later.

This journal is © The Royal Society of Chemistry 2017

Open Access Article. Published on 18 October 2017. Downloaded on 6/14/2026 12:01:09 PM.
This article is licensed under a Creative Commons Attribution-NonCommercial 3.0 Unported Licence.

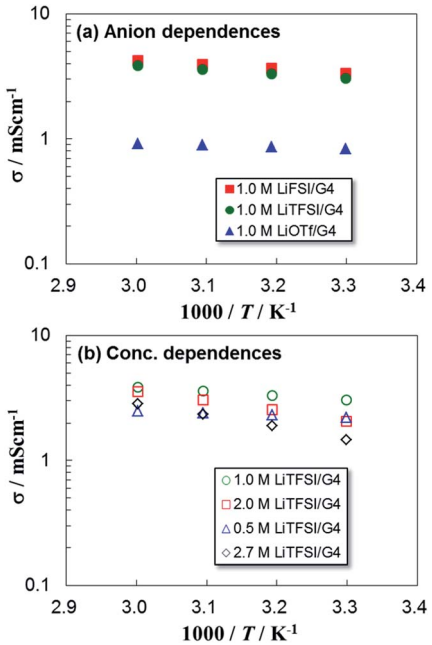

Fig. 2 Comparison of the temperature dependences of ionic conductivity σ for 1.0 M G4-based electrolytes with (a) three kinds of Li salts with different anions (OTf^-, $TFSI^-$, and FSI^-) and (b) a common Li salt (LiTFSI) at different concentrations (0.5, 1.0, 2.0, and 2.7 M). The values for 1.0 M LiTFSI/G4 and LiFSI/G4 almost overlap.

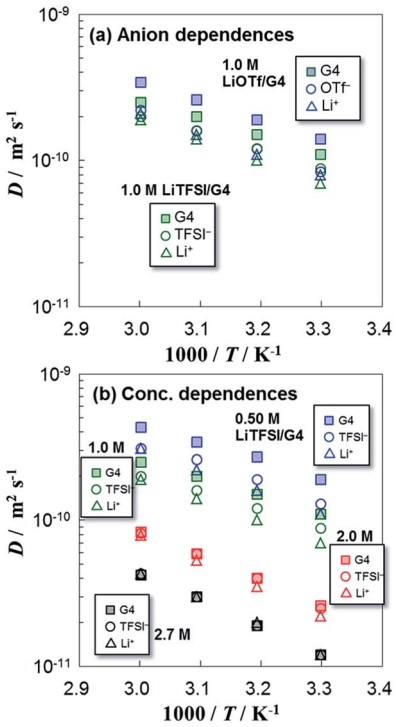

Fig. 3 Typical temperature dependences of self-diffusion coefficients D for (a) 1.0 M G4-based electrolytes containing LiOTf and LiTFSI salts and (b) a common LiTFSI salt with different concentration.

σ was defined by eqn (1),

$$\sigma = \sum_j q_j \times \mu_j \times n_j, \quad (1)$$

where q, μ, and n are the charge, mobility and number of carrier ions per specific volume, respectively; the suffix j corresponds to Li^+ or anions. Here, to consider μ of each carrier ion, we separately measured D of Li^+, anions, and G4 solvent by PGSE-NMR. Typical Arrhenius-type plots for the G4-based electrolytes containing 1.0 M LiOTf and LiTFSI are shown in Fig. 3. The D values of the LiOTf electrolyte are larger than those of the LiTFSI one; within the same electrolyte, $D_{G4} > D_{anion} > D_{Li^+}$ across the entire temperature range. The numerical data including those for the LiFSI electrolyte are summarized in Tables 1 (D) and 2 (η) in ESI.† The temperature dependences essentially followed Arrhenius-type behavior, indicating that the ions are transported by flow of the G4 solvent and the anions move more easily than Li^+ in the electrolytes. However, the difference between D of the chemical species became smaller as the concentration of Li salts increased (Fig. 3(b)). This trend was similar to those reported for electrolytes for Li-ion batteries (LIBs)[24] and was also in good agreement with those of solvate ionic liquids.[19,20,32] The orders of magnitude of D were LiOTf > LiFSI > LiTFSI and 0.5 M > 1.0 M > 2.0 M > 2.7 M for the type of Li salt and its concentration, respectively. These trends do not correspond to those for σ. This indicates that σ is strongly influenced by n in the electrolytes.

From the slopes of the plots of the temperature dependences of D, the activation energies E_a were estimated for the electrolyte systems, as shown in Table 1. For all electrolytes, E_a values were from 0.23 to 0.37 eV. E_a of the glyme electrolytes were relatively high compared with those of LIB electrolytes but on a similar scale, as same as those for a G3-based electrolyte.[33] This means that all chemical species transport in a similar manner in these electrolytes.

From the D values of Li+ and anions, the apparent transference numbers of Li^+ t_{Li^+} were calculated using eqn (2):

$$t_{Li^+} = D_{Li^+}/(D_{Li^+} + D_{anion}). \quad (2)$$

The results at 303 K are shown in Table 1 (t_{Li^+} at each temperature are summarized in S1†). All t_{Li^+} values were between 0.41 and 0.51, which are relatively high compared with those reported for organic carbonate electrolytes used in LIBs.[24]

In general, σ and D values are strongly related to the viscosity of the electrolyte. D of electrolyte solutions is known to increase with decreasing viscosity. Fig. 4(a) and (b) display the

Table 1 Activation energies E_a obtained from Arrhenius-type plots of D for ions and G4 solvents and the transference number of Li^+ t_{Li^+} at 303 K for 1.0 M glyme-based electrolytes

Electrolyte solution	D_{G4} E_a/eV	D_{Li^+} E_a/eV	D_{anion} E_a/eV	t_{Li^+}
1.0 M LiOTf/G4	0.23	0.26	0.30	0.49
1.0 M LiTFSI/G4	0.24	0.24	0.29	0.44
1.0 M LiFSI/G4	0.24	0.29	0.27	0.43
0.50 M LiTFSI/G4	0.23	0.26	0.30	0.46
2.0 M LiTFSI/G4	0.34	0.34	0.37	0.47
2.7 M LiTFSI/G4	0.37	0.37	0.37	0.50

Open Access Article. Published on 18 October 2017. Downloaded on 6/14/2026 12:01:09 PM.
This article is licensed under a Creative Commons Attribution-NonCommercial 3.0 Unported Licence.

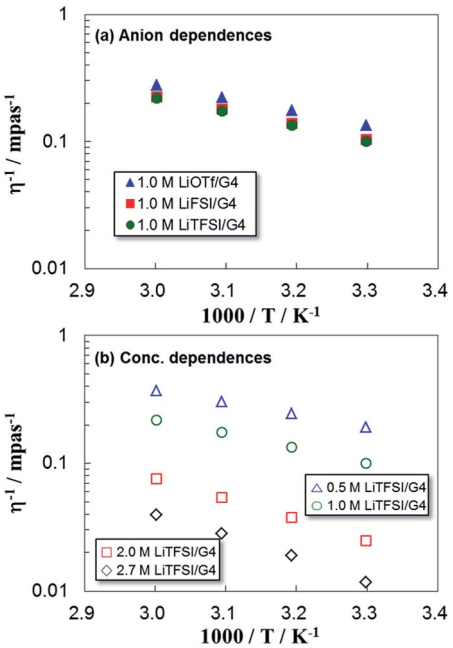

Fig. 4 Temperature dependences of inverse viscosity η^{-1} for 1.0 M G4-based electrolytes containing (a) three kinds of Li salts with different anions and (b) LiTFSI salt at different concentrations.

temperature dependences of inverse viscosity η^{-1} for 1.0 M G4-based electrolyte solutions containing different Li salts and different concentrations of LiTFSI salt, respectively. The η^{-1} values for all electrolytes followed the trends of temperature dependences: LiOTf > LiFSI > LiTFSI and 0.50 M > 1.0 M > 2.0 M > 2.7 M. Because we used G4 as a solvent in all the samples, η^{-1} was mainly affected by the dissolved salt. The η^{-1} values showed good correspondence with those of D.

Fig. 5 shows ρ of the electrolytes as a function of temperature. The ρ values decreased linearly with rising temperature: LiTFSI > LiFSI > LiOTf and 2.7 M > 2.0 M > 1.0 M > 0.5 M. This is also in good agreement with the trend of η, implying that an electrolyte with smaller ρ exhibits lower η and higher D. These parameters are usually reflected by the mutual interactions between ions and solvent in the electrolytes. In the following section, we analyze the ion transport mechanism from the viewpoints of both μ and n in the glyme electrolytes, including the mutual interactions between the ions and G4 solvent.

Discussion

To observe the effect of μ of the carrier ions on σ, the σ values are plotted against the sum of $(D_{Li^+} + D_{anion})$ in Fig. 6(a) and (b) for different Li salts and different concentrations of LiTFSI, respectively. The σ values increased with $(D_{Li^+} + D_{anion})$ for all the electrolytes. Except for the LiOTf electrolyte, the Li^+ and anion diffusion constants clearly influenced σ. The σ values depended on the counteranions with the order FSI^- > $TFSI^-$ ≫ OTf^-. For the LiOTf electrolyte, σ values were small compared with those of the other Li salts and the change was quite small even when the temperature increased. This indicates that the degree of dissociation was low and decreased with rising temperature. Regarding the dependence on Li salt concentration, $(D_{Li^+} + D_{anion})$ drastically decreased with increasing concentration. However, σ did not decrease; instead, it was almost constant over a similar range. This suggests that the dissociation degree α was basically

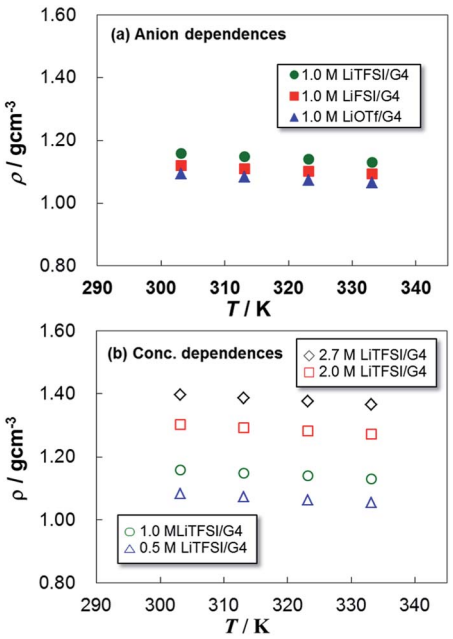

Fig. 5 Comparison of the temperature dependences of density ρ for 1.0 M G4-based electrolytes containing (a) three kinds of Li salts with different anions and (b) LiTFSI salt at different concentrations.

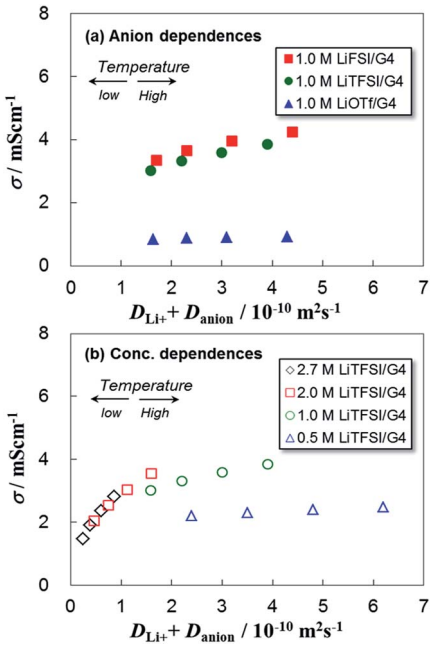

Fig. 6 Plots of ionic conductivity σ against the sum of $(D_{cation} + D_{anion})$ for (a) three kinds of Li salts with different anions and (b) LiTFSI salt at different concentrations.

This journal is © The Royal Society of Chemistry 2017

Open Access Article. Published on 18 October 2017. Downloaded on 6/14/2026 12:01:09 PM.
This article is licensed under a Creative Commons Attribution-NonCommercial 3.0 Unported Licence.

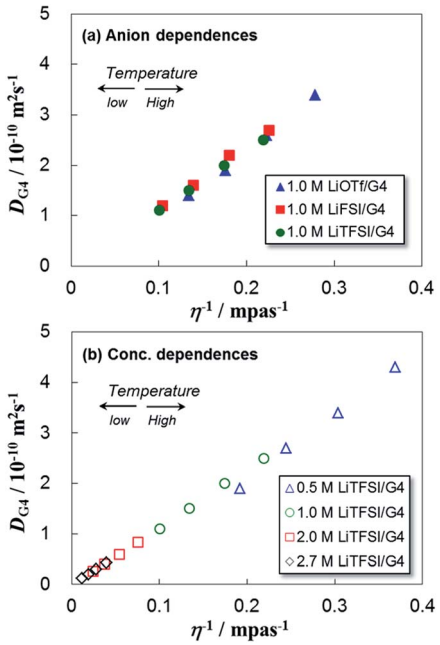

Fig. 7 Plots of solvent self-diffusion coefficients D_{G4} against the inverse viscosity η^{-1} for 1.0 M G4-based electrolytes in (a) three kinds of Li salt with different anions and (b) LiTFSI salt at different concentrations.

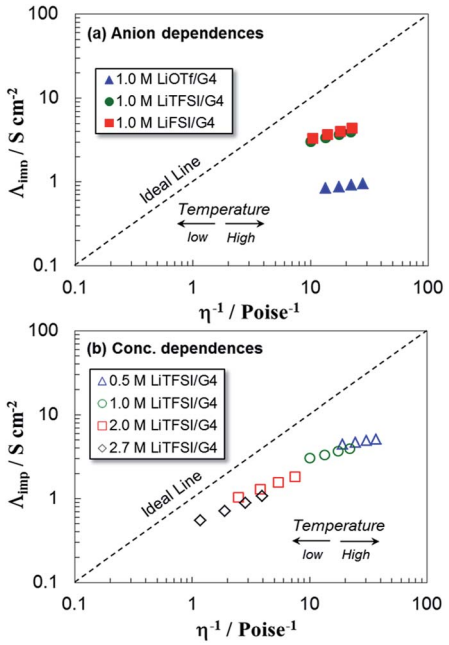

Fig. 8 Walden plots for G4-based electrolytes with (a) three kinds of Li salts with different anions and (b) LiTFSI salt at different concentrations.

enhanced by increasing the Li salt concentration, as reported by Watanabe's group.[19,20,32]

As mentioned above, ion transport in glyme electrolytes occurs *via* a vehicle mechanism. The relationship between D and η can therefore be defined by the Stokes–Einstein equation[24,28] as follows:

$$D = kT/c\pi\eta r_{ion}, \quad (3)$$

where k is Boltzmann's constant, T is temperature (K), η is the viscosity of the electrolyte (Pa s^{-1}), r_{ion} is the Stokes (solvated ion) radius (m) and c is a constant, which ranges between 4 and 6 for slip and stick boundary conditions, respectively.[34] Eqn (3) implies that an electrolyte with lower η exhibits higher D of the solvent. Fig. 7 shows D of G4, D_{G4}, plotted against η^{-1} of the electrolytes. For all the electrolytes, D_{G4} increased proportionally with η^{-1} according to eqn (3). This trend was also clearly confirmed for the concentration dependence of LiTFSI, as shown in Fig. 7(b).

In eqn (3), c and η are assumed to be the same for the ions and G4, so r_{ion}/r_{G4} is simply defined as eqn (4):[26]

$$r_{ion}/r_{G4} = D_{G4}/D_{ion}. \quad (4)$$

The r_{ion}/r_{G4} value represents the effective radius of the diffusing ion in the electrolyte because the PGSE-NMR method gives average values of D of the ions and G4. Table 2 shows the ion radius relative to that of G4 (r_{ion}/r_{G4}) for the six electrolytes. All the r_{ion}/r_{G4} values were larger than those determined from the van der Waals radii of the ions. This implies that either Li^+ strongly interacts with G4 to form a solvated $Li^+(G4)_x$ species or counter-anions contribute to the formation of ion pairs. As a result, Li^+ diffuses more slowly than the anions in the electrolytes. In addition, the r_{Li}/r_{G4} and r_{anion}/r_{G4} values for the LiOTf electrolyte were relatively larger than those of the electrolytes with other salts. This indicates that Li^+ forms a larger amount of ion pairs and larger solvated ion structures in the presence of both G4 and OTf^-. Also, the r_{ion}/r_{G4} values decreased with increasing Li salt concentration. This indicates that the dissociation degree increased with rising concentration. In the glyme electrolytes, the mutual interactions between ions and solvent are relatively strong and influence the ion transport behavior by changing the solvation structures. As shown by eqn (1), σ of solution electrolytes is also influenced by n. In the following section, we conducted analyses using Walden plots and the Nernst–Einstein equation to elucidate the effect of n on σ.[28]

Fig. 8(a) and (b) illustrate the Walden plots for electrolytes with different Li salts and LiTFSI at different concentrations, respectively. Here, σ was converted to molar conductivity Λ_{imp}

Table 2 Ionic radius relative to G4 (r_{ion}/r_{G4}) in the G4-based electrolytes at 303 K calculated using eqn 4

Species	LiOTf (1.0 M)	LiTFSI (1.0 M)	LiFSI (1.0 M)	LiTFSI (0.50 M)	LiTFSI (2.0 M)	LiTFSI (2.7 M)
Anion	1.7	1.3	1.2	1.5	1.0	1.0
Li^+	1.8	1.6	1.6	1.7	1.2	1.0

Open Access Article. Published on 18 October 2017. Downloaded on 6/14/2026 12:01:09 PM.
This article is licensed under a Creative Commons Attribution-NonCommercial 3.0 Unported Licence.

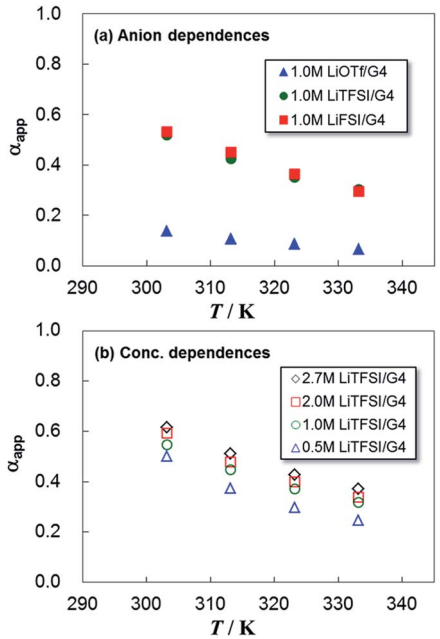

Fig. 9 Plots of the degree of dissociation α_{app} for glyme-based electrolytes with (a) three kinds of Li salts with different anions and (b) LiTFSI at different concentrations.

using the ρ values in Fig. 5. The Walden plots deviated downward from the ideal line. For the Li salts, the deviation became much larger with the order of LiOTf $\gg$ LiTFSI $\geq$ LiFSI. All the Li salts exhibited larger deviation with increasing temperature, indicating a decrease in the degree of dissociation of the salts. As for the concentration dependence of LiTFSI, a higher Li salt concentration gave a smaller deviation than those of lower ones. This means that the glyme-based electrolytes form more stable Li^+ solvation structures at high concentration, such as a 1 : 1 ratio of glyme to Li^+ (corresponding to 2.7 M).[19,20,32] Therefore, the contribution of n to σ increases with rising concentration especially at lower temperatures. In contrast, lower Li salt concentration and higher temperature are considered to increase the contribution of μ to σ.

Molar ionic conductivity Λ_{NMR} can be calculated from the self-diffusion coefficients (D_+, D_-) by the Nernst–Einstein equation as follows:

$$\Lambda_{NMR} = Ne^2(D_+ + D_-)/kT, \quad (5)$$

where N is the number of isolated ions per specific volume. Eqn (5) holds for electrolytes in which ions are perfectly dissociated (such as in an infinitely dilute solution). From the D_+ and D_- values determined from PGSE-NMR measurements, the experimental Λ_{NMR} values were calculated for the six electrolytes. PGSE-NMR data provided the average D values for all ions, including isolated and paired ones. However, NMR measurements cannot distinguish charged (isolated) ions from paired ions, so the experimental Λ_{NMR} includes all the diffusion species. This has been confirmed by infinite dilution of Li^+ organic electrolyte solutions, for which eqn (5) exactly holds.[25] In practical electrolytes, the calculated experimental Λ_{NMR} is always larger than Λ_{imp} at all temperatures. The apparent degree of ion dissociation α_{app} in the electrolytes can be determined from eqn (6):[24–26]

$$\alpha_{app} = \Lambda_{imp}/\Lambda_{NMR}. \quad (6)$$

Fig. 9 shows the temperature dependences of the α_{app} values for the lithium salts. At 303 K, α_{app} is the largest for LiFSI, with the order LiFSI $\geq$ LiTFSI $\gg$ LiOTf. Generally, α_{app} values are insensitive to temperature for solution electrolytes. However, the glyme-based electrolytes exhibited a gradual decrease in α_{app} with increasing temperature. This is in good agreement with the results of the Walden plots and is attributed to the increase of ligand exchange rate caused by raising the temperature. In fact, the higher concentration of LiTFSI electrolyte exhibited higher α_{app} over the whole temperature range than α_{app} of the lower concentration of LiTFSI.

The Walden plots and α_{app} values indicate that ion dissociation is higher for LiFSI and LiTFSI salts than for LiOTf. The magnitude of deviation in the Walden plots agrees well with the order of ion dissociation α_{app}: LiFSI $\geq$ LiTFSI $\gg$ LiOTf. This trend is similar to those estimated from Λ_{imp} and the limiting molar conductivity Λ_0 for the solvate ionic liquids of [Li(G3)]X and [Li(G4)]X (X: anions) reported by Watanabe and coworkers.[32] The changes in Li salt concentration and temperature revealed the interaction strength of G4 with Li^+, which is not strong compared with those of organic carbonate solvents such as PC and EC. However, an increase in n enhanced the interaction in the [Li^+(G4)]X complexes. By increasing n, this order also agreed well with that of σ. Namely, σ of the glyme electrolytes is more closely related to n than μ.

The μ and n of the carrier ions are strongly related to the physical parameters η, ρ, and D, so it is necessary to understand

Table 3 Interaction energy ΔE between Li^+–anion of the salts and G4–Li^+ for solvation[a]

Interaction	$E(Li^+)$/au	E(anion, G4)/au	E(Li^+–anion, G4–Li^+)/au	ΔE/eV
Li^+–OTf^-	−7.28491780	−961.730421	−969.241731	−6.10
Li^+–$TFSI^-$ (*cis*)	−7.28491780	−1827.61042	−1835.11844	−5.97
Li^+–$TFSI^-$ (*trans*)	−7.28491780	−1827.61042	−1835.12077	−6.04
Li^+–FSI^- (*cis*)	−7.28491780	−1351.90295	−1359.40749	−5.88
Li^+–FSI^- (*trans*)	−7.28491780	−1351.90295	−1359.40583	−5.83
G4–Li^+	−7.28491780	−770.586715	−778.038815	−4.39

[a] The basis set superposition error (BSSE) for ΔE is corrected by the counterpoise method.

This journal is © The Royal Society of Chemistry 2017

Open Access Article. Published on 18 October 2017. Downloaded on 6/14/2026 12:01:09 PM.
This article is licensed under a Creative Commons Attribution-NonCommercial 3.0 Unported Licence.

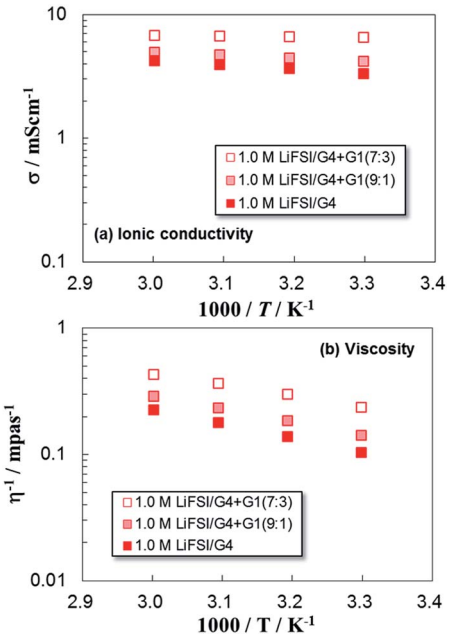

Fig. 10 Plots of (a) ionic conductivity σ and (b) viscosity η for 1.0 M LiFSI/G4 + G1 (9 : 1, 7 : 3) together with those of 1.0 M LiFSI/G4.

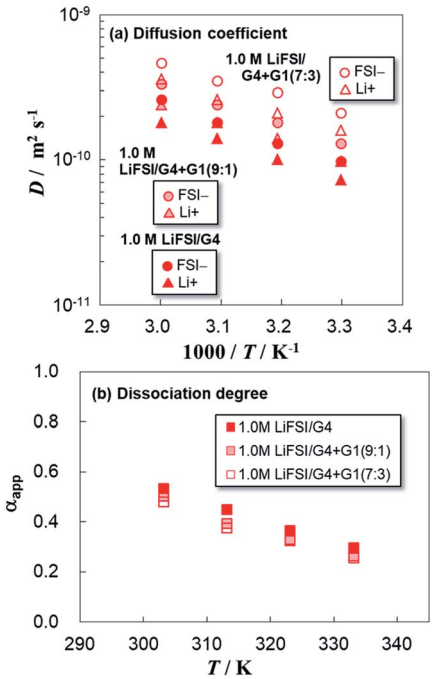

Fig. 11 Plots of self-diffusion coefficients D and dissociation degree α_{app} for 1.0 M LiFSI/G4 + G1 (9 : 1, 7 : 3) together with those of 1.0 M LiFSI/G4.

the mutual interactions between Li^+–anion and G4–Li^+. Here, we calculated these two interaction energies ΔE using a DFT calculation based on supermolecule method.[22,23] When an interaction occurs, for example, between M1 and M2, the intermolecular interaction energy, ΔE, is calculated as the difference between the total energy of the dimer [E(M1 − M2)] and the sum of the total energies of monomers [E(M1) and E(M2)] as shown in eqn (7):

$$\Delta E = E(\mathrm{M1} - \mathrm{M2}) - [E(\mathrm{M1}) + E(\mathrm{M2})]. \quad (7)$$

The optimized geometries calculated for the Li^+–anion and G4–Li^+ complexes are shown in Fig. 1 in ESI.† The total energies, E(M1), E(M2), and E(M1 − M2), and the calculated ΔE values between Li^+–anion and G4–Li^+ are summarized in Table 3. The order of magnitude of ΔE is LiOTf > LiTFSI > LiFSI even if the geometry of $TFSI^-$ and FSI^- anions is changed between *cis* and *trans* structures, which means that FSI^- is the mostly likely to dissociate from Li^+ among the supporting salts.

Considering the solvation energy of Li^+ by G4, ΔE for the G4–Li^+ interaction is also summarized in Table 3. In general, ΔE of G4–Li^+ is relatively large (−4.39 eV), which stabilizes the solvation structure. The ΔE value (solvation energy) is at a similar level to those of Li^+–anion interactions, but it is not high enough for full dissociation of the salts, even if considering the G4–anion interaction. Therefore, the Li salts were not fully dissociated in the glyme electrolytes. However, the FSI^- and $TFSI^-$ anions exhibited a tendency for higher dissociation, which led to enhanced σ: this is in good agreement with the results of Walden plots and α_{app} of the electrolytes. Consequently, the LiFSI electrolyte exhibited the highest σ of those investigated. We therefore have to find Li salts with smaller dissociation energies to improve salt dissociation, which will increase n of the glyme electrolytes. The ionic radii of the solvated Li^+ and anions are also important for glyme electrolytes because they affect μ in a similar manner to that in conventional Li salt electrolytes, such as 1.0 M $LiPF_6$/EC + DEC for LIBs.[27] Therefore, FSI^- also has an advantage from the viewpoint of diffusion radius because of its smaller ion size and higher dissociation degree than those of the other anions.

The above results indicate that σ of glyme-based electrolytes depends on both μ and n. In particular, improvement of the dissociation degree of Li salts is quite important because of the lower solvation energy of glyme than those of other carbonate-type solvents for LIBs. In addition, the dissociation degree increases with Li salt concentration. Next, we tried to design new electrolyte systems using DME (G1) as the solvent. G1 has similar a dielectric constant (7.2) and lower η (0.455 mPas) compared with those of G4 (7.9 and 4.05 mPas, respectively). Therefore, keeping a similar dissociation degree and lowering η for the glyme electrolyte are expected. Here, 1.0 M LiFSI/G4 + G1 (9 : 1 or 7 : 3 molar ratio) and concentrated (conc.) LiFSI/G1 (3.5 or 5.0 M) systems were examined. Fig. 10(a) and (b) show the temperature dependences of σ and η for 1.0 M LiFSI/G4 + G1,

Table 4 Activation energies E_a determined from Arrhenius-type plots of D for ions and G4 solvents and transference number of Li^+ t_{Li^+} at 303 K for 1.0 M LiFSI/G4 + G1 electrolytes

Electrolyte solution	D_{G1} E_a/eV	D_{Li^+} E_a/eV	D_{anion} E_a/eV	t_{Li^+}
1.0 M LiFSI/G4 + G1 (9 : 1)	—	0.26	0.27	0.43
1.0 M LiFSI/G4 + G1 (7 : 3)	—	0.23	0.22	0.43

Open Access Article. Published on 18 October 2017. Downloaded on 6/14/2026 12:01:09 PM.
This article is licensed under a Creative Commons Attribution-NonCommercial 3.0 Unported Licence.

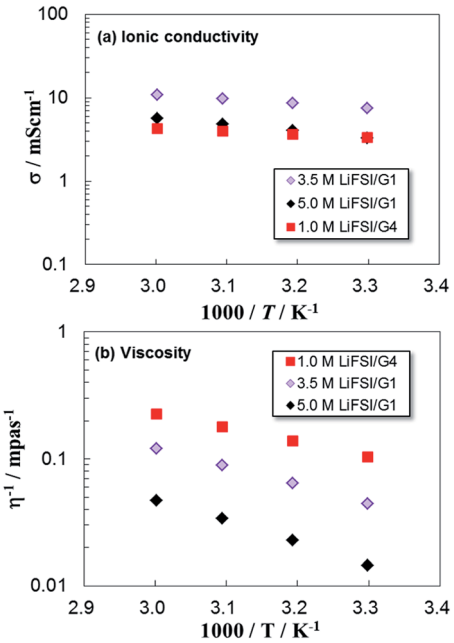

Fig. 12 Plots of (a) ionic conductivity σ and (b) viscosity η for concentrated LiFSI/G1 (3.5, 5.0 M) together with those of 1.0 M LiFSI/G4.

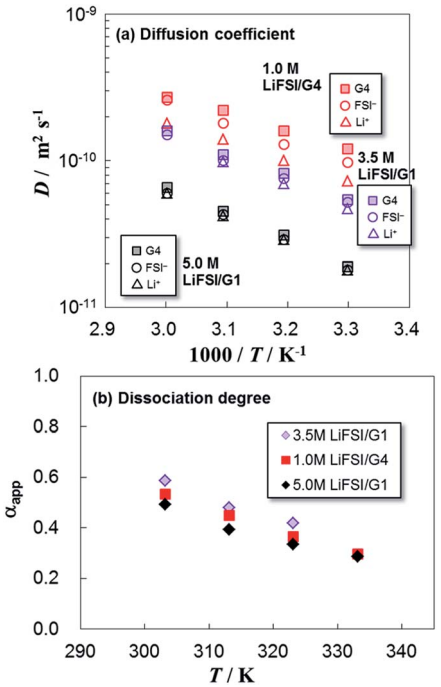

Fig. 13 Plots of self-diffusion coefficients D and dissociation degree α_{app} for conc. LiFSI/G1 (3.5, 5.0 M) together with 1.0 M LiFSI/G4.

respectively. The σ values increased with the content of G1 in the electrolytes. This is attributed to the decrease of η. To consider μ and n, D and α_{app} values are plotted against temperature in Fig. 11. The D values of ions drastically increased with rising G1 content in the electrolyte, while α_{app} decreased slightly with increasing G1 content. As a result, σ increased to 6.5 mS cm^{-1}, which is *ca.* twice that of the pristine electrolyte (3.3 mS cm^{-1}); *i.e.*, 1.0 M LiFSI/G4. The activation energies of ions estimated from D values also decreased and relatively high t_{Li^+} were maintained (Table 4), indicating increases of μ. Therefore, lowering η using the G1 solvent with a similar dielectric constant and lower η to those of G4 is one way to effectively improve σ of glyme electrolyte systems.

Fig. 12 depicts σ and η for the conc. LiFSI/G1 (3.5 or 5.0 M) system. Both conc. G1-based electrolytes exhibited higher σ values than that of 1.0 M LiFSI/G4 electrolyte despite the lower η^{-1} values. This suggests that n increases with Li salt concentration. In particular, σ of 3.5 M LiFSI/G1 was 3.3 mS cm^{-1}, which is twice that of 1.0 M LiFSI/G4, as well as 1.0 M LiFSI/G4 + G1 (7 : 3) mentioned above. Considering the μ and n values, both 3.5 and 5.0 M LiFSI/G1 electrolytes exhibited lower D values because of their higher η compared with those of 1.0 M LiFSI/G4 (Fig. 13), but similar or higher α_{app} values were obtained for the conc. G1-based electrolytes, indicating the enhancement of n. Therefore, σ of conc. glyme electrolytes was strongly controlled by n. Because of the intrinsic low η of G1, the η^{-1} and D values were relatively high compared with those of the G4-based electrolytes. This concept is connected to the recent conc. Li salt electrolytes with low viscosity.[35] The transference number of Li^+, t_{Li^+}, also became high upon increasing Li salt concentration and the r_{Li^+}/r_{G1} value was close to 1.0 (Table 5). This implies that LiFSI dissociates well in the conc. electrolytes and each Li^+ is solvated by one or two G1 molecules. In fact, the Li salt concentrations of 3.5 and 5.0 M correspond to the molar ratios of Li^+ to G1 of 1 : 2 and 1 : 1, respectively. Further investigation is needed to elucidate the properties of conc. electrolytes including the other solvents.

Table 5 Activation energies E_a from Arrhenius-type plots of D for ions and G1 solvents, transference number of Li^+ t_{Li^+} and ionic radius relative to G1 r_{Li^+}/r_{G1} at 303 K for conc. LiFSI/G1 electrolytes

Electrolyte solution	D_{G1} E_a/eV	D_{Li^+} E_a/eV	D_{FSI^-} E_a/eV	t_{Li^+}	r_{Li^+}/r_{G1}
3.5 M LiFSI/G1	0.31	0.31	0.30	0.44	1.2
5.0 M LiFSI/G1	0.36	0.35	0.35	0.50	1.1

Conclusions

In this study, we discussed ion transport in glyme-based electrolytes obtained using three Li salts (LiOTf, LiTFSI, and LiFSI) and two glyme solvents (G4, G1). The μ values were clearly dominated by the kind of Li salt. Namely, the Lewis basicity and hardness of anions influenced the interaction strength between Li^+ and anions (Li salt dissociation), Li^+ and glymes (Li^+ solvation), and determined η of electrolytes related to D. ΔE were estimated by DFT calculations based on the supermolecule method and provided useful information to design new electrolyte systems. As a result, one of the most effective determination factors for high σ was n for the glyme-based electrolytes with low dielectric constant. Using a smaller ether solvent with similar dielectric constant such as G1 was demonstrated to be

This journal is © The Royal Society of Chemistry 2017

Open Access Article. Published on 18 October 2017. Downloaded on 6/14/2026 12:01:09 PM.
This article is licensed under a Creative Commons Attribution-NonCommercial 3.0 Unported Licence.

quite effective to enhance σ while keeping η relatively low. From the obtained knowledge, we demonstrated two methods, *i.e.*, improvement of μ and n by using 1.0 M LiFSI/G4 + G1 (9 : 1 and 7 : 3 molar ratio) and conc. LiFSI/G1 (3.5 and 5.0 M) electrolyte systems. As expected, both electrolytes successfully exhibited improved σ values (3.3 S cm^{-2}) that were twice that of 1.0 M LiFSI/G4. In addition, the conc. Li salt electrolytes are expected to widen the electrochemical window; *i.e.*, improve electrochemical stability.[19–21,32] This is also attractive as an electrolyte property for use in next-generation batteries such as LABs that need a relatively high potential (over 4.2 V) at the air electrode for the charge process. However, conc. glyme electrolytes are expensive because of their high content of Li salts. To realize industrial production, we need to further investigate the use of other solvents with low η and wide electrochemical windows, which effectively enhance σ of glyme-based electrolytes by raising μ and n. Such research is in progress.

Conflicts of interest

There are no conflicts to declare.

Acknowledgements

This work was partly supported by each of JST Project for the ALCA-SPRING and MEXT Programs for the Development of Environmental Technology using Nanotechnology and the scientific technology human resource development grant, Japan. We thank Dr K. Hayamizu from the University of Tsukuba for fruitful advice.

References

1 P. G. Bruce, S. A. Freunberger, L. J. Hardwick and J. M. Tarascon, *Nat. Mater.*, 2011, **11**, 19.
2 K. M. Abraham and Z. A. Jiang, *J. Electrochem. Soc.*, 1996, **143**, 1.
3 F. Mizuno, S. Nakanishi, Y. Kotani, S. Yokoishi and H. Iba, *Electrochemistry*, 2010, **78**, 403.
4 B. D. McCloskey, D. S. Bethune, R. M. Shelby, G. Girishkumar and A. C. Luntz, *J. Phys. Chem. Lett.*, 2011, **2**, 1161.
5 W. Xu, K. Xu, V. V. Viswanathan, S. A. Towne, J. S. Hardy, J. Xiao, Z. Nie, D. Hu, D. Wang and J.-G. Zhang, *J. Power Sources*, 2011, **196**, 9631.
6 V. S. Bryantsev, V. Giordani, W. Walker, M. Blanco, S. Zecevic, K. Sasaki, J. Uddin, D. Addison and G. V. Chase, *J. Phys. Chem. A*, 2011, **115**, 12399.
7 S. A. Freunberger, *J. Am. Chem. Soc.*, 2011, **133**, 8040.
8 D. Aurbach, M. Daroux, P. Faguy and E. Yeager, *J. Electroanal. Chem.*, 1991, **297**, 225.
9 I. Gunasekara, S. Mukerjee, E. J. Plichta, M. A. Hendrickson and K. M. Abraham, *J. Electrochem. Soc.*, 2015, **162**(6), A1055.
10 S. A. Freunberger, *Angew. Chem., Int. Ed.*, 2011, **50**, 8609.
11 B. D. McCloskey, D. S. Bethune, R. M. Shelby, G. Grishkumar and A. C. S. Luntz, *J. Phys. Chem. Lett.*, 2011, **2**, 1161.
12 W. Xu, J. Xiao, D. Wang, J. Zhang and J.-G. Zhang, *Electrochem. Solid-State Lett.*, 2010, **13**, A48.
13 Y. Chen, S. A. Freunberger, Z. Peng, O. Fontaine and P. G. Bruce, *Nat. Chem.*, 2013, **5**, 489.
14 H.-D. Lim, H. Song, J. Kim, H. Gwon, Y. Bae, K.-Y. Park, J. Hong, H. Kim, T. Kim, Y. H. Kim, X. Lepró, R. Ovalle-Robles, R. H. Baughman and K. Kang, *Angew. Chem., Int. Ed.*, 2014, **53**, 3926.
15 W.-J. Kwak, D. Hirshberg, D. Sharon, H.-J. Shin, M. Afri, J.-B. Park, A. Garsuch, F. F. Chesneau, A. A. Frimer, D. Aurbach and Y.-K. Sun, *J. Mater. Chem. A*, 2015, **3**, 8855.
16 C. M. Burke, R. Black, I. R. Kochetkov, V. Giordani, D. Addison, L. F. Nazar and B. D. McCloskey, *ACS Energy Lett.*, 2016, **1**(4), 747.
17 J. Uddin, V. S. Bryantsev, V. Giordani, W. Walker, G. V. Chase and D. Addison, *J. Phys. Chem. Lett.*, 2013, **4**, 3760.
18 L. Carbone, M. Gobet, J. Peng, M. Devany, B. Scrosati, S. Greenbaum and J. Hassoun, *J. Power Sources*, 2015, **299**, 460.
19 H. Moon, T. Mandai, R. Tatara, K. Ueno, A. Yamazaki, K. Yoshida, S. Seki, K. Dokko and M. Watanabe, *J. Phys. Chem. C*, 2015, **119**(8), 3957.
20 H.-M. Kwon, M. L. Thomas, R. Tatara, Y. Oda, Y. Kobayashi, A. Nakanishi, K. Ueno, K. Dokko and M. Watanabe, *ACS Appl. Mater. Interfaces*, 2017, **9**(7), 6014.
21 J. Qain, W. A. Henderson, W. Xu, P. Bhattacharya, M. Engelhard, O. Borodin and J. G. Zhang, *Nat. Commun.*, 2015, **6**, 6362.
22 C. Møller and M. S. Plesset, *Phys. Rev.*, 1934, **46**, 618.
23 M. Head-Gordon, J. A. Pople and M. J. Frisch, *Chem. Phys. Lett.*, 1988, **153**, 503.
24 K. Hayamizu, Y. Aihara, S. Arai and C. G. Martinez, *J. Phys. Chem. B*, 1999, **103**, 519.
25 Y. Aihara, K. Sugimoto, W. S. Price and K. Hayamizu, *J. Chem. Phys.*, 2000, **113**, 1981.
26 K. Hayamizu, E. Akiba, T. Banno and Y. Aihara, *J. Chem. Phys.*, 2002, **117**, 5929.
27 K. Hayamizu, *J. Chem. Eng. Data*, 2012, **57**, 2012.
28 M. Saito, S. Kawaharasaki, K. Ito, S. Yamada, K. Hayamizu and S. Seki, *RSC Adv.*, 2017, **7**, 14528.
29 M. J. Frisch, G. W. Trucks, H. B. Schlegel, G. E. Scuseria, M. A. Robb, J. R. Cheeseman, G. Scalmani, V. Barone, B. Mennucci, G. A. Petersson, H. Nakatsuji, M. Caricato, X. Li, H. P. Hratchian, A. F. Izmaylov, J. Bloino, G. Zheng, J. L. Sonnenberg, M. Hada, M. Ehara, K. Toyota, R. Fukuda, J. Hasegawa, M. Ishida, T. Nakajima, Y. Honda, O. Kitao, H. Nakai, T. Vreven, J. A. Montgomery Jr, J. E. Peralta, F. Ogliaro, M. Bearpark, J. J. Heyd, E. Brothers, K. N. Kudin, V. N. Staroverov, R. Kobayashi, J. Normand, K. Raghavachari, A. Rendell, J. C. Burant, S. S. Iyengar, J. Tomasi, M. Cossi, N. Rega, J. M. Millam, M. Klene, J. E. Knox, J. B. Cross, V. Bakken, C. Adamo, J. Jaramillo, R. Gomperts, R. E. Stratmann, O. Yazyev, A. J. Austin, R. Cammi, C. Pomelli, J. W. Ochterski, R. L. Martin, K. Morokuma, V. G. Zakrzewski, G. A. Voth, P. Salvador, J. J. Dannenberg, S. Dapprich, A. D. Daniels, Ö. Farkas, J. B. Foresman, J. V. Ortiz, J. Cioslowski and D. J. Fox, *Gaussian 09, Revision B.01*, Gaussian, Inc., Wallingford CT, 2009.

Open Access Article. Published on 18 October 2017. Downloaded on 6/14/2026 12:01:09 PM.
This article is licensed under a Creative Commons Attribution-NonCommercial 3.0 Unported Licence.

30 B. J. Ransil, *J. Chem. Phys.*, 1961, **34**, 2109.
31 S. Boys and F. Bernardi, *Mol. Phys.*, 1970, **19**, 553.
32 K. Ueno, K. Yoshida, M. Tsuchida, N. Tachikawa, K. Dokko and M. Watanabe, *J. Phys. Chem. B*, 2012, **116**, 11323.
33 L. Carbone, D. D. Lecce, M. Gobet, S. Munoz, M. Devany, S. Greenbaum and J. Hassoun, *ACS Appl. Mater. Interfaces*, 2017, **9**, 17085.
34 H. Evey, A. G. Bishop, M. Forsyth and D. R. MacFarlane, *Electrochim. Acta*, 2000, **45**, 1279.
35 Y. Yamada and A. Yamada, *J. Electrochem. Soc.*, 2015, **162**(14), A2406.

This journal is © The Royal Society of Chemistry 2017